Small GTP-binding protein Ran is regulated by posttranslational lysine acetylation

Susanne de Boor[1], Philipp Knyphausen[1], Nora Kuhlmann, Sarah Wroblowski, Julian Brenig, Lukas Scislowski, Linda Baldus, Hendrik Nolte, Marcus Krüger, and Michael Lammers[2]

Institute for Genetics and Cologne Excellence Cluster on Cellular Stress Responses in Aging-Associated Diseases, University of Cologne, 50931 Cologne, Germany

Edited by Alan R. Fersht, Medical Research Council Laboratory of Molecular Biology, Cambridge, United Kingdom, and approved June 5, 2015 (received for review March 26, 2015)

Ran is a small GTP-binding protein of the Ras superfamily regulating fundamental cellular processes: nucleo-cytoplasmic transport, nuclear envelope formation and mitotic spindle assembly. An intracellular Ran•GTP/Ran•GDP gradient created by the distinct subcellular localization of its regulators RCC1 and RanGAP mediates many of its cellular effects. Recent proteomic screens identified five Ran lysine acetylation sites in human and eleven sites in mouse/rat tissues. Some of these sites are located in functionally highly important regions such as switch I and switch II. Here, we show that lysine acetylation interferes with essential aspects of Ran function: nucleotide exchange and hydrolysis, subcellular Ran localization, GTP hydrolysis, and the interaction with import and export receptors. Deacetylation activity of certain sirtuins was detected for two Ran acetylation sites in vitro. Moreover, Ran was acetylated by CBP/p300 and Tip60 in vitro and on transferase overexpression in vivo. Overall, this study addresses many important challenges of the acetylome field, which will be discussed.

Ran | lysine acetylation | genetic code expansion concept | nucleus | nuclear cytosolic transport

The small GTP-binding protein Ran (Ras-related nuclear) is involved in nucleo-cytoplasmic transport processes, nuclear envelope formation, and the formation of the mitotic spindle (1). Ran, furthermore, has a variety of cytosolic functions and is involved in the cross-talk with the actin cytoskeleton. As a member of the Ras superfamily, Ran is structurally composed of a fold known as the G-domain (GTP-binding domain), a central six-stranded β-sheet that is surrounded by α-helices. Ras-family members bind to GTP and GDP nucleotides with high picomolar affinity. However, only in the GTP-bound form and the switch I- and switch II-loops adopt a stable conformation. Ran has been structurally characterized in great detail, including different nucleotide states and various protein complexes (2–4).

In interphase cells, about 90% of cellular Ran is nuclear, and only a minor proportion is cytosolic (5). The localization of the guanine-nucleotide exchange factor (GEF) RCC1 (Regulator of chromosome condensation 1) at the nuclear chromatin and the RanGAP (RanGTPase-activating protein) at the cytosolic site of the nuclear pore creates a gradient of Ran•GTP in the nucleus and Ran•GDP in the cytosol (6–8).

In the nucleus, Ran•GTP binds to exportins such as CRM1 (Chromosome region maintenance 1) to transport cargo proteins containing a nuclear export signal (NES) into the cytosol (3, 9, 10). Ran•GTP, furthermore, binds to Importin-β•cargo complexes to release the cargo in the nucleus (11–15). In the cytosol, the Importin•Ran•GTP complexes, as well as the ternary exportin•Ran•GTP-cargo complexes, dissociate on binding of RanBP1 and subsequent GTP hydrolysis catalyzed by RanGAP (16, 17). The Ran transport cycle closes by translocation of Ran•GDP to the nucleus by the nuclear transport factor 2 (NTF2) (4, 17–20). Many of these Ran interactions also play important roles in mitotic spindle assembly and nuclear envelope formation.

Several subfamilies of the Ras superfamily are posttranslationally modified by phosphorylation, ubiquitylation, and/or lipidation. Recently, Ras was found to be lysine acetylated at K104, regulating its oncogenicity by affecting the conformational stability of switch II (21). By contrast, Ran is neither targeted to cellular membranes by lipid modifications nor regulated by phosphorylation. However, Ran has recently been shown to be lysine acetylated at five distinct sites in human (K37, K60, K71, K99, and K159) (22). The lysine acetylation sites were found independently by several studies in different species using highly sensitive quantitative MS (22–26). K37 is located within switch I, K60 in the β3-strand preceding switch II, K71 in switch II, K99 in α-helix three (α3), and K159 in α5 C-terminal to the 150-SAK-152 motif interacting with the nucleotide base (Fig. 1*A*). Due to the localization of these lysine acetylation sites, it appears reasonable that they might interfere with essential Ran functions.

Here, we present the first, to our knowledge, comprehensive study on the impact of posttranslational lysine acetylation on Ran function using a combined synthetic biological, biochemical, and biophysical approach. We analyzed Ran activation and inactivation by RCC1 and RanGAP, intrinsic GTP exchange and hydrolysis, Ran localization, and cargo import and export complex formation. Finally, we provide evidence for Ran being a target of certain lysine acetyltransferases and deacetylases in vitro. Our data reveal general mechanisms how lysine acetylation regulates protein functions taking Ran as a model system. Finally, we discuss the implications of recent high-throughput proteomic studies discovering thousands of acetylation sites in a variety of different organisms.

Significance

The small GTPase Ran plays fundamental roles in cellular processes such as nucleo-cytoplasmic transport, mitotic spindle formation, and nuclear envelope assembly. Recently, Ran was found to be lysine acetylated, among others, in functionally important regions such as switch I and switch II. Using the genetic code expansion concept we show that lysine acetylation affects many important aspects of Ran function such as RCC1-catalyzed nucleotide exchange, intrinsic nucleotide hydrolysis, import/export complex formation, and Ran subcellular localization. Finally, we present evidence for a regulation of Ran acetylation by sirtuin deacetylases and lysine acetyltransferases.

Author contributions: S.d.B., P.K., and M.L. designed research; S.d.B., P.K., N.K., S.W., J.B., L.S., L.B., and M.L. performed research; S.d.B., P.K., N.K., S.W., J.B., H.N., M.K., and M.L. analyzed data; and S.d.B., P.K., and M.L. wrote the paper.

The authors declare no conflict of interest.

This article is a PNAS Direct Submission.

[1]S.d.B. and P.K. contributed equally to this work.

[2]To whom correspondence should be addressed. Email: michael.lammers@uni-koeln.de.

This article contains supporting information online at www.pnas.org/lookup/suppl/doi:10.1073/pnas.1505995112/-/DCSupplemental.

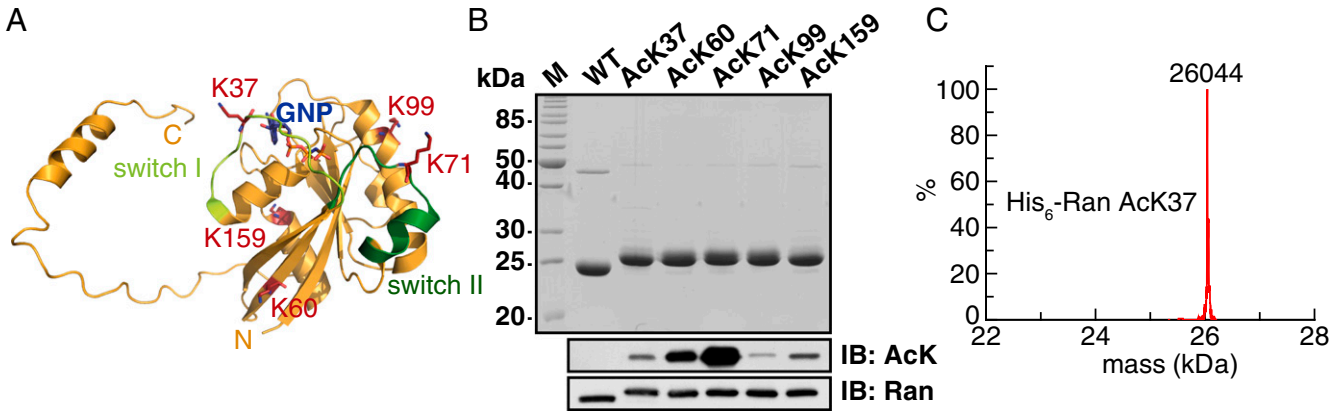

Fig. 1. Incorporation of *N*-(ε)-acetyl-L-lysine into Ran using the genetic code expansion concept. (*A*) Ribbon representation of Ran (yellow) and position of the five lysine acetylation sites (red) studied here (PDB ID code 1K5D). $K37^R$ in switch I (light green), $K60^R$ in β3, $K71^R$ in switch II (dark green), $K99^R$ in α3 and $K159^R$ in α5. (*B*) Final purity of the recombinantly expressed WT Ran and lysine acetylated proteins shown by SDS/PAGE (*Top*). Immunoblotting (IB) of Ran proteins using a specific anti–acetyl-lysine (ab21623) antibody (*Middle*). The antibody differentially recognizes the different acetylation sites in Ran and does not detect Ran_{WT}. The immunoblotting using an anti–Ran-antibody shows equal loading. (*C*) Acetyl-lysine is quantitatively incorporated at position 37 in Ran. The corresponding theoretical molecular mass of the nonacetylated His_6-Ran protein is 26,001 Da; the acetyl group has a molecular weight of 42 Da.

Results

Site-Specific Incorporation of *N*-(ε)-Acetyl-Lysine Using the Genetic Code Expansion Concept. To site-specifically incorporate *N*-(ε)-acetyl-L-lysine (AcK) into Ran, we used a synthetically evolved aminoacyl-tRNA synthetase/$tRNA_{CUA}$ (aa-syn/$tRNA_{CUA}$) pair from *Methanosarcina barkeri* expressed in *Escherichia coli* [genetic code expansion concept (GCEC)] (27, 28). Using this system, we produced full-length recombinant Ran proteins, monoacetylated at five distinct sites (K37, K60, K71, K99, and K159) in high purity and yields suitable for biophysical studies (Fig. 1 *A* and *B*). As confirmed by electrospray ionization (ESI) MS and immunoblotting (Fig. 1 *B* and *C* and Fig. S1 *A* and *B*), the obtained material is homogenously and quantitatively acetylated, i.e., in contrast to material prepared by purified acetyltransferases, it allows a site-specific study. Differences in the detection sensitivity of the AcK-specific antibody (anti-AcK) can most likely be attributed to the structural context and amino acid residues adjacent to each Ran-AcK site (Fig. 1*B*).

Ran Acetylation Impairs the RCC1-Catalyzed Nucleotide Exchange Reaction. First, we performed single turnover stopped-flow experiments to assess the impact of Ran acetylation on RCC1-catalyzed nucleotide exchange rates. The Ran proteins were loaded with fluorescently labeled mantGDP (500 nM) and mixed with increasing concentrations of RCC1 (0.0195–40 μM) in the presence of an excess of unlabeled GTP (25 μM). The primary data were fitted to a single exponential function to result in the observed rate constants k_{obs}. These k_{obs} values were plotted against the RCC1 concentration following a hyperbolic function (29). The hyperbolic fit resulted in the rate of dissociation of the nucleotide from the ternary RCC1•Ran•mantGDP complex, k_{-2} (Fig. 2 *B* and *C* and Fig. S2*A*). Ran acetylation on K37 moderately and K71 and K99 strongly reduce the RCC1-catalyzed nucleotide dissociation rate, with Ran AcK99 showing a nearly 10-fold reduction (k_{-2}: Ran_{WT} 12.8 s^{-1}, AcK37 9.3 s^{-1}, AcK71 5.9 s^{-1}, AcK99 1.3 s^{-1}). By contrast, Ran AcK60 (k_{-2}: 16.5 s^{-1}) and AcK159 (k_{-2}: 14.7 s^{-1}) slightly increase the dissociation rates compared with nonacetylated Ran.

Ran Acetylation Interferes with RCC1 Binding. To assess the impact of Ran acetylation on RCC1 affinity and interaction thermodynamics, we performed equilibrium isothermal titration calorimetry (ITC) experiments with GDP- and GppNHp-loaded Ran (Table S1). All reactions (except for Ran AcK99) are driven by both favorable reaction enthalpy and entropy of comparable magnitudes at 25 °C. Consistent with our nucleotide exchange data shown above, acetylation on $K71^R$ and $K99^R$ (superscript R: Ran) had the strongest impact on RCC1 binding. Acetylation on $K71^R$ increases the binding affinity toward both GDP- (6-fold) and GppNHp- (20-fold) loaded Ran. Measurements with Ran AcK99 had to be performed at 30 °C because of a weak heat signal at 25 °C, indicating an altered binding mechanism. Under these conditions, the affinity in the GDP-bound state was reduced threefold from 560 to 1,400 nM (Table S1). Taken together, we conclude that Ran acetylation at lysines 71 and 99 severely disturbs RCC1-catalyzed nucleotide exchange.

These findings can be related to available structural data [Protein Data Bank (PDB) ID code 1I2M] (9). RCC1 forms a seven-bladed β-propeller structure (Fig. 2*A*) and mediates the nucleotide exchange reaction by targeting helix α3, switch II, and the P-loop in Ran (9, 30). On binding to RCC1, $K99^R$ on α3 becomes relocalized and interacts with $D128^G$ and $N181^G$ (superscript G: RCC1-GEF). $K71^R$ interacts with $N268^G$ and $H304^G$ and is also in interaction distance to the P-loop $K18^R$ (Fig. 2*A*). Moreover, it was reported earlier that $K71^R$ and $F72^R$ are most important for the interaction with RCC1, whereas mutations of $D182A^G$ and $H304A^G$ significantly affect the RCC1 k_{cat} (9). Our findings suggest that acetylation of lysines 71 or 99 affects major interaction sites of Ran and RCC1 (switch II and α3) and ultimately impacts on RCC1 interaction and catalysis.

Impact of Ran Acetylation on Nucleotide Hydrolysis and the Interaction with RanGAP and RanBP1.

Ran acetylation only marginally affects the intrinsic nucleotide hydrolysis rate. The intrinsic GTP hydrolysis rate of Ran is very slow (5.4×10^{-5} s^{-1} at 37 °C) and would not be of biological significance if not 10^5-fold (2.1 s^{-1} at 25 °C) accelerated by RanGAP (31). We speculated that acetylation of lysines in the switch regions ($K37^R$ and $K71^R$) modulates intrinsic and/or RanGAP-mediated GTP hydrolysis. However, we found that lysine acetylation on Ran only marginally affects the intrinsic and GAP-catalyzed GTP hydrolysis rates (Fig. 2 *D* and *E*). Only for AcK71 did we observe a 1.5-fold increase of the intrinsic hydrolysis rate from 5.8 to 8.9 s^{-1} at 37 °C (Fig. 2*E*). K71 in Ran is in close proximity to $Q69^R$, which is needed for positioning of the water molecule for GAP-catalyzed GTP hydrolysis. This $Q69^R$ might become reoriented on acetylation of $K71^R$ to accelerate the intrinsic GTP hydrolysis rate.

Acetylation of Ran on K159 reduces its affinity toward RanBP1. RanBP1 increases the affinity of RanGAP toward Ran•GTP from 7 to 2 μM

and toward Ran•GDP from 100 to 2 μM by inducing a GTP-like conformation in Ran•GDP (32, 33). We determined thermodynamic profiles of the Ran-RanBP1 interaction in both nucleotide states, GDP and GppNHp, by ITC (Table S1). RanBP1 binds to Ran•GDP with 7.1 μM and to Ran•GppNHp with 3 nM. Acetylation of Ran only marginally affects the interaction to both active and inactive Ran except for Ran AcK159. Ran•GppNHp AcK159 shows a more than 10-fold reduced affinity toward RanBP1 compared with nonacetylated Ran•GppNHp (3 to 33 nM). $K159^{R}$ is not directly contacting RanBP1, suggesting an indirect mechanism leading to the decrease in RanBP1 affinity (PDB ID code 1RRP). Also, the nucleotide-dependent difference observed for the Ran AcK159•RanBP1 interaction needs further investigation.

Interaction of Ran with RanGAP in the presence of RanBP1. When Ran•GTP is bound to transport receptors, it is protected from RanGAP activity. Only on binding of RanBP1 is Ran released from transport complexes, allowing for RanGAP to induce GTP hydrolysis (16, 34). We thus analyzed by ITC whether Ran acetylation affects the Ran•GppNHp•RanGAP interaction in the presence of RanBP1 (Table S1). In fact, we did not observe a heat signal for the interaction of RanGAP and Ran•GppNHp alone but only in the presence of RanBP1. In these assays, RanGAP bound to a preformed complex of Ran•GppNHp•RanBP1 with 0.5 μM. Surprisingly, we observed an *N* value of 0.5 when RanGAP was used as a titrant for Ran•RanBP1 and of 1.5 when titration was performed vice versa (Table S1). This stoichiometry suggests that, at the concentrations used for ITC, one binding site of the Ran•RanBP1 complex is not available or, less likely, that RanGAP can bind two complexes.

Interestingly, acetylation of $K99^{R}$ lowers the affinity to 17 μM (34-fold reduction). $K99^{R}$ is positioned toward an acidic patch in RanGAP (superscript GAP: RanGAP) comprising residues $E336^{GAP}$-$E345^{GAP}$ (PDB ID code 1K5D). Acetylation of $K99^{R}$ might electrostatically and sterically interfere with this interaction, possibly explaining the loss in affinity. Because acetylation of $K99^{R}$ did not affect the GAP-mediated hydrolysis directly (Fig. 2*D*), we tested whether this would be different in the presence of RanBP1. However, we could not detect any effect of Ran acetylation on RanGAP-mediated nucleotide hydrolysis in the presence of RanBP1 (Fig. S2*B*).

Acetylation of lysine 71 in Ran abolishes binding to NTF2. Ran•GDP binds to NTF2 in the cytosol and is transported back into the nucleus, which closes the Ran transport cycle (35). As visible in the NTF2•Ran•GDP structure, $K71^{R}$ forms a salt bridge to

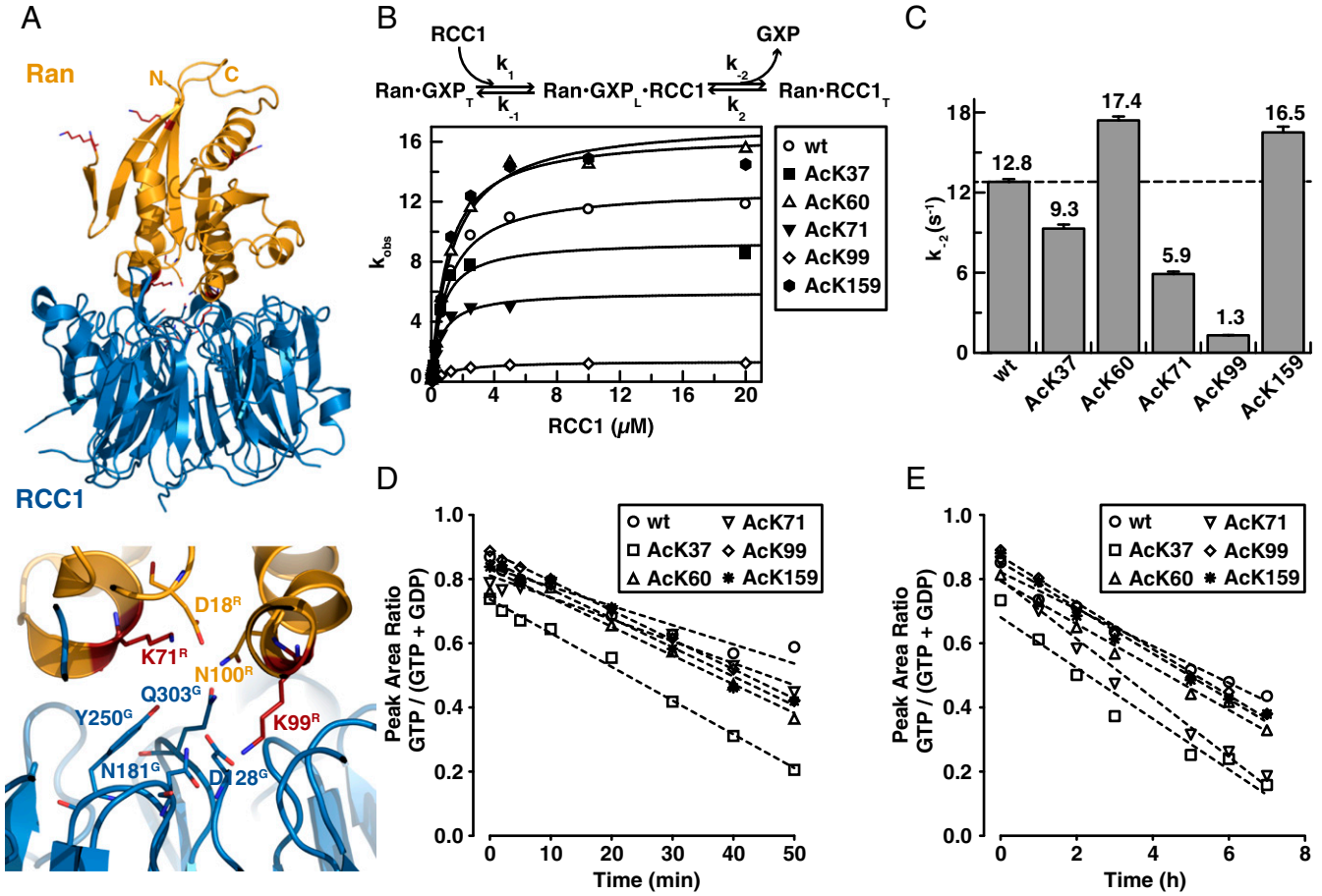

Fig. 2. Acetylation of Ran interferes with RCC1 catalyzed nucleotide exchange and RanGAP-catalyzed and intrinsic nucleotide hydrolysis. (*A*) Structure of the Ran•RCC1-complex and close up of the binding interface, showing interactions of Ran K71/K99 as described in the text (PDB ID code 1I2M). RCC1 (blue), Ran (yellow), acetylation sites (red). (*B*) Pseudo–first-order kinetics of nucleotide exchange rates of 500 nM Ran (final concentration) titrated with increasing RCC1 concentrations (0.0195–20 μM). The scheme shows that Ran•GDP with tightly bound nucleotide (GXP: GTP or GDP; subscript: T) binds RCC1 first loosely in a ternary Ran•GXP•RCC1-complex (subscript: L), and in the second step, the nucleotide is released with a dissociation rate k_{-2} to result in a tight Ran•RCC1 complex. (*C*) The hyperbolic fit resulted in the rate of nucleotide dissociation from the ternary Ran•GDP•RCC1 complex, k_{-2}. (*D*) RanGAP-stimulated nucleotide hydrolysis on Ran. GTP hydrolysis rates were examined by HPLC determining the GTP/(GTP + GDP) ratio as a function of time. The acetylation does not alter GAP-catalyzed nucleotide hydrolysis on Ran. (*E*) Intrinsic nucleotide hydrolysis on Ran and acetylated Ran. The rates were determined as described in *D*. Ran AcK71 leads to a 1.5-fold increase in the intrinsic GTP hydrolysis rate, whereas the other Ran AcKs are similar to WT Ran.

$D92/D94^N$ (superscript N: NTF2) in NTF2 (PDB ID code 1A2K; Fig. 3*A*) (4). The analysis of the NTF2•Ran•GDP interaction by ITC revealed that nonacetylated and acetylated Ran binds NTF2 with affinities in the middle nanomolar range (Ran_{WT} 260 nM; Fig. 3*D* and Table S1). Ran acetylation on K71, however, abolishes this interaction. This effect was also confirmed by analytical size exclusion chromatography (SEC). To test the impact of $K71^R$ acetylation on the cellular Ran localization, we constructed the Ran K71Q and K71R mutants to mimic acetylation and to conserve the charge at $K71^R$, respectively. Before cell culture experiments, the validity of the acetylation mimetics was confirmed by ITC and analytical SEC (Fig. S2*C*). Analogous to Ran AcK71, K71Q did not bind NTF2 as judged by ITC (Fig. 3*D*). In the case of K71R, the NTF2 binding was 15-fold reduced compared with WT Ran (Fig. 3*D* and Table S1), reflecting the charge conservation in combination with steric restrictions.

We expressed the K to Q and K to R mutants of all five Ran acetylation sites in HeLa cells. Ran_{WT} and the majority of mutants predominantly localize to the nucleus (Fig. 3 *B* and *C*). By contrast, Ran K71Q is almost depleted from the nucleus, in accordance with our biophysical data, demonstrating the failure of complex formation between Ran and NTF2. Notably, $K99R^R$ also shows significant cytosolic distribution, although the mutation does not affect NTF2 binding (Table S1). Taken together, our data suggest that acetylation at $K71^R$ and $K99^R$ would affect Ran localization most drastically. Although mislocalization of Ran K71Q seems linked to loss of NTF2 binding, a different mechanism has to be considered for the mislocalization of Ran K99R.

Ran Acetylation in Import and Export Processes.

Ran acetylation increases the affinity toward Importin-β by altering the interaction dynamics. We characterized the effect of Ran acetylation on the interaction with the major import receptor Importin-β. None of the Ran acetylation sites negatively interfered with Importin β-binding. Ran AcK37, AcK99, and AcK159 lead to a 9- to 15-fold increase in Importin-β binding affinity as judged by ITC (K_D: Ran_{WT} 160 nM; AcK37 11 nM; AcK99 18 nM; AcK159 16 nM; Fig. 4*D*).

To interpret the affinity differences in the context of interaction dynamics, we analyzed the impact of Ran-lysine acetylation on the association kinetics to Importin-β by stopped-flow experiments (Fig. 4 *A*–*C* and Fig. S3*A*). The association rates obtained for WT Ran and Importin-β (k_{on}: 15.8 $mM^{-1}{\cdot}s^{-1}$) agree with reported values (k_{on}: 12 $mM^{-1}{\cdot}s^{-1}$) (13). The acetylation of Ran at $K37^R$ leads to a nearly fivefold increase in the Importin-β association rate (k_{on}: 50 $mM^{-1}{\cdot}s^{-1}$), whereas it is only marginally increased for AcK159 (k_{on}: 22 $mM^{-1}{\cdot}s^{-1}$). All of the other Ran acetylation sites AcK60/71/99 lead to a slight reduction in the association rates to Importin-β (k_{on}: AcK60 5 $mM^{-1}{\cdot}s^{-1}$; AcK71 11 $mM^{-1}{\cdot}s^{-1}$; AcK99 6 $mM^{-1}{\cdot}s^{-1}$). Taken together, the presented interaction studies demonstrate that Ran acetylation at different lysine residues alters the interaction dynamics with Importin-β by influencing both association and dissociation rates. In the case of acetylated Ran on lysine 37, 99, and 159, this results in noticeably increased binding affinities as determined by ITC. The acetylation might induce a Ran conformation more potent to bind Importin-β or alternatively impact on Importin-β binding by influencing the interaction kinetics. However, to finally judge this, we would need further structural information.

Ran acetylation interferes with export complex formation. Next, we tested whether Ran acetylation would interfere with export complex formation using the export receptor CRM1 and the CRM1 substrate snurportin 1 (Spn1) as a model system. In accordance with previous studies, CRM1 and Spn1 interact with an apparent affinity of 1.2 μM, whereas direct titration of Ran•GppNHp and CRM1 did not produce a heat signal in ITC (Fig. S3*B*, *Upper Left*) (36). However, titration of Ran•GppNHp onto a preformed

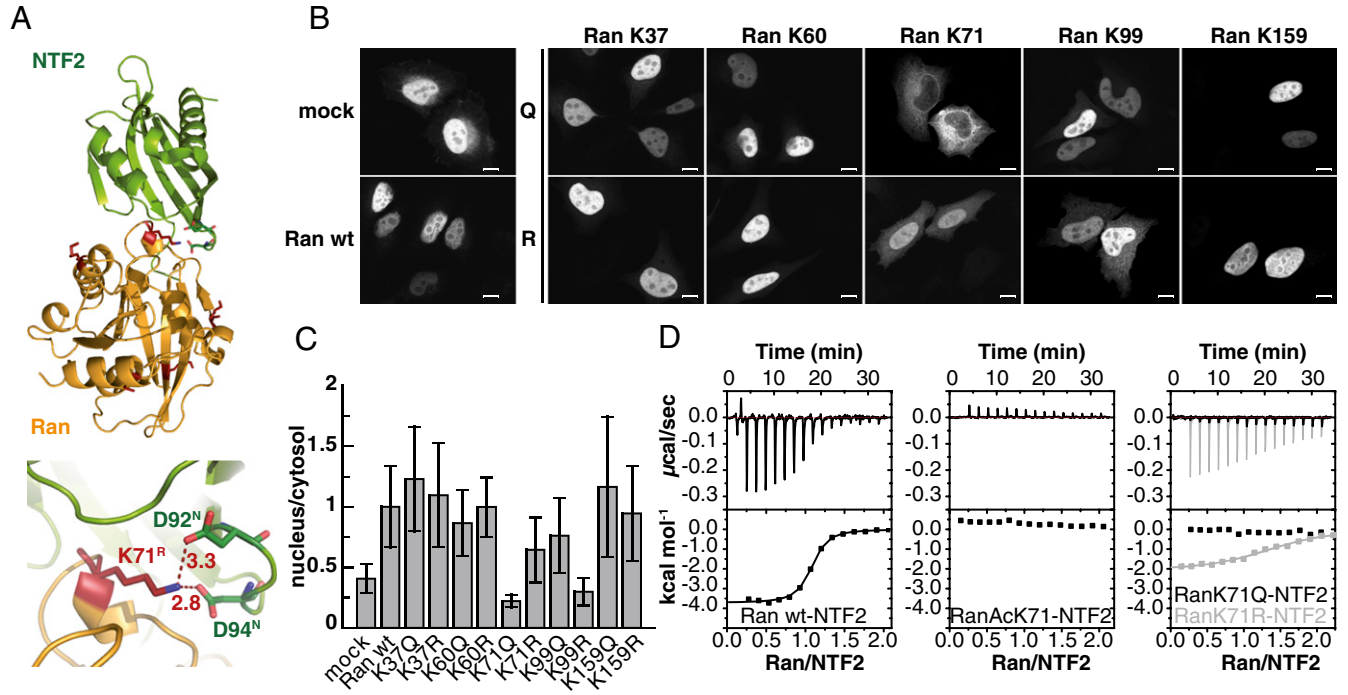

Fig. 3. Ran AcK71 abolishes nuclear localization of Ran by blocking NTF2 binding. (*A*) Ribbon representation of the NTF2-Ran•GDP complex (PDB ID code 1A2K). K71 of Ran forms a salt bridge to D92/D94 in NTF2. Shown are the distances in Angstroms. (*B*) EGFP fluorescence of the Ran-EGFP K to Q and K to R mutants in HeLa cells. Ran localizes mainly to the nucleus for WT and all mutants except for Ran K71Q and K99R, which are primarily cytosolic. (*C*) Quantification of subcellular Ran by measurement of the EGFP fluorescence in the nucleus and the cytosol. As shown in *B*, Ran K71Q and K99R localize to the cytosol, whereas the others are predominantly nuclear. (*D*) Thermodynamic characterization of the interaction of NTF2 and Ran, Ran AcK71, Ran K71Q (acetylation mimic), and Ran K71R (charge conserving) by ITC. K71Q and AcK71 abolish binding toward NTF2.

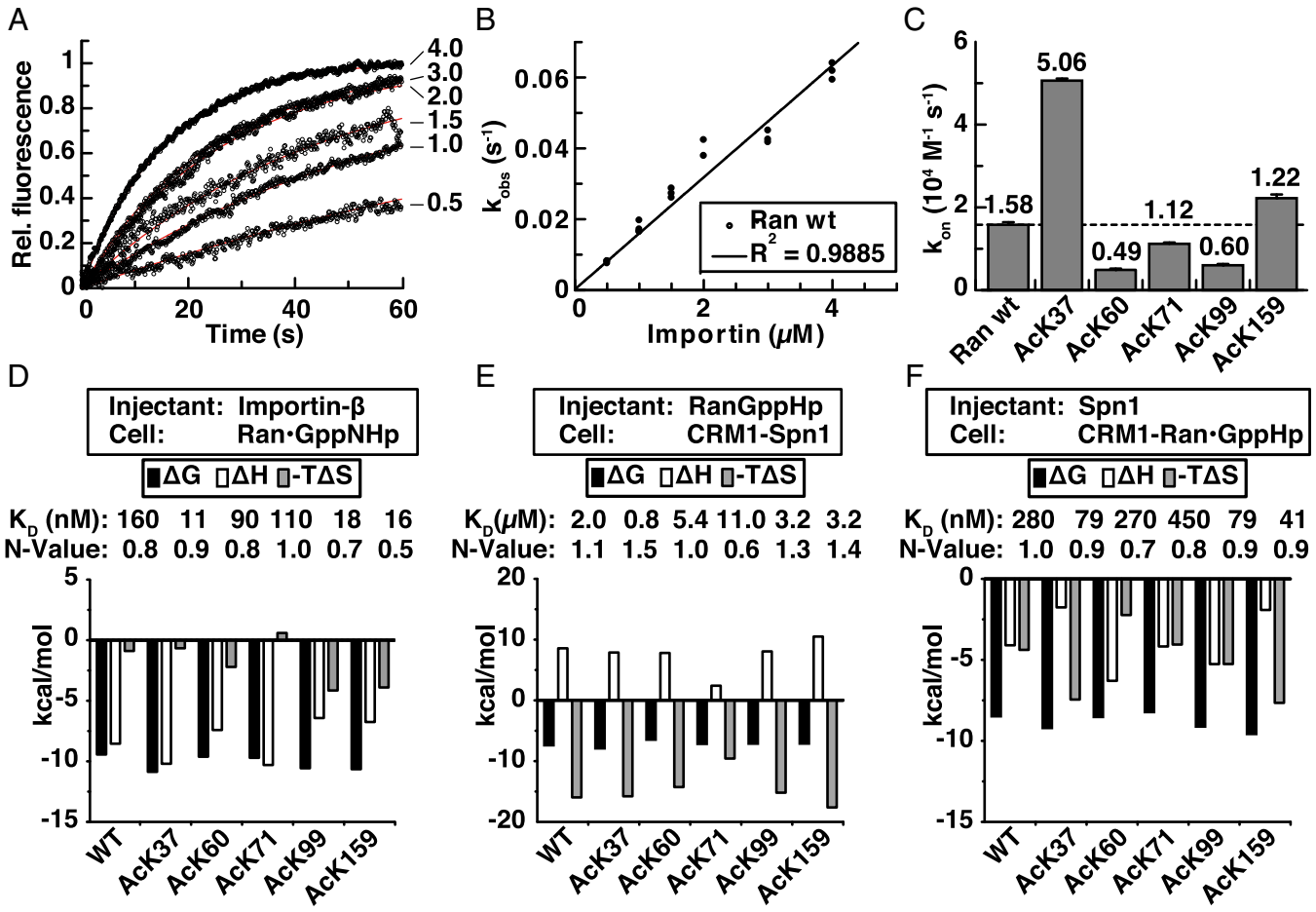

Fig. 4. Acetylation of Ran in import and export complex formation. (*A*) Association kinetics of Ran•mantGppNHp WT (100 nM final) and increasing concentrations of Importin-β (final: 0.5–4 μM) as determined by stopped-flow. The kinetics were fitted single exponentially to result in the observed rate constants, k_{obs}. (*B*) Determination of the Ran•mantGppNHp-Importin-β association rate constant. The obtained k_{obs} values were plotted against the Importin-β concentration. The linear fit resulted in the association rate constant, k_{on}. (*C*) Comparison of the association rates for Importin-β-Ran_{WT} and the acetylated Ran proteins. Ran AcK37 increases the association rate fivefold. (*D*) Thermodynamics of the Importin-β (268 μM) and Ran•GppNHp (40 μM) interaction as determined by ITC. Ran AcK37, AcK99, and AcK159 increase the affinity toward Importin-β. (*E*) Thermodynamics of the interaction of Ran•GppNHp (200 μM) titrated onto a Crm1•Spn1-complex (20/40 μM) determined by ITC. Ran AcK71 decreases the Ran•GppNHp affinity to the complex fivefold. (*F*) Thermodynamic profile of the interaction of 200 μM Spn1 titrated onto a preformed Crm1•Ran•GppNHp-complex (20/40 μM) as determined by ITC. Ran AcK37, AcK99, and AcK159 increase the binding affinity of Spn1 to the preformed complex.

CRM1•Spn1 complex revealed an entropically driven reaction with an affinity of 2 μM, indicating that Spn1 influences the thermodynamics of Ran-CRM1 binding (Fig. S3*B*, *Upper Right*). Interestingly, the interaction of Spn1 with CRM1 is also influenced by the presence of Ran•GppNHp, leading to an increased affinity of 280 nM (Fig. 4*F* and Fig. S3*B*, *Lower Right*). These observations fit to the current understanding of export complex formation, in which cargo proteins and Ran•GTP cooperatively bind to CRM1 (see model in Fig. S3*B*) (18).

The binding of Ran•GppNHp to CRM1•Spn1 was largely unaffected by acetylation. Only acetylation at $K71^R$ reduces the affinity toward the CRM1•Spn1 complex fivefold (Fig. 4*E*). We reasoned that acetylation of Ran might influence the ability of Ran to promote binding of Spn1 to CRM1. To test this hypothesis, we titrated Spn1 onto preformed complexes of CRM1 and acetylated Ran. In this scenario, acetylation at K37, K99, and K159 led to a four- to sevenfold increased affinity of Spn1 to CRM1 (K_D: 40–80 nM; Fig. 4*F*). Because the affinities and the relative cellular concentrations of proteins determine how Ran•GTP•CRM1 export cargo interactions occur within the cell, acetylation of Ran might impact on the order of consecutive steps involved in export complex formation.

Ran is deacetylated at AcK37 by Sirt1, -2, and -3 and by Sirt2 at AcK71 in vitro. To identify possible deacetylases for Ran, we performed an in vitro dot-blot screen of all 11 mammalian classical (HDAC1-11) and 7 sirtuin deacetylases (Sirt1-7) using the acetylated Ran proteins as substrates (Fig. S4 *A* and *B*). To normalize the enzymatic activities used in the assay, all enzymes were tested in a fluor-de-lys assay beforehand (Fig. S4*C*). None of the classical deacetylases showed a striking deacetylase activity against any of the Ran acetylation sites (Fig. S4*A*). However, we identified a strong Ran deacetylation at AcK37 by Sirt1, -2, and -3 and at AcK71 only by Sirt2. An immunoblot assay confirmed that Sirt1, -2, and -3 deacetylate Ran AcK37 and Ran AcK71 is exclusively deacetylated by Sirt2 (Fig. 5 *A* and *B*). The reaction is dependent on the presence of the sirtuin-cofactor NAD^+, and it can be inhibited by the addition of the sirtuin-specific inhibitor nicotinamide (NAM) (Fig. 5*A*).

Following the deacetylation by Sirt1-3 over a time course of 90 min revealed that Sirt2 shows highest activity toward Ran AcK37, leading to complete deacetylation after 5 min while taking at least 30 min for Sirt1 and Sirt3 under the conditions used. Deacetylation at AcK71 did again occur only with Sirt2 but at a slower rate compared with AcK37 as substrate (Fig. 5*B*). Next, we wondered whether the nucleotide state or the presence

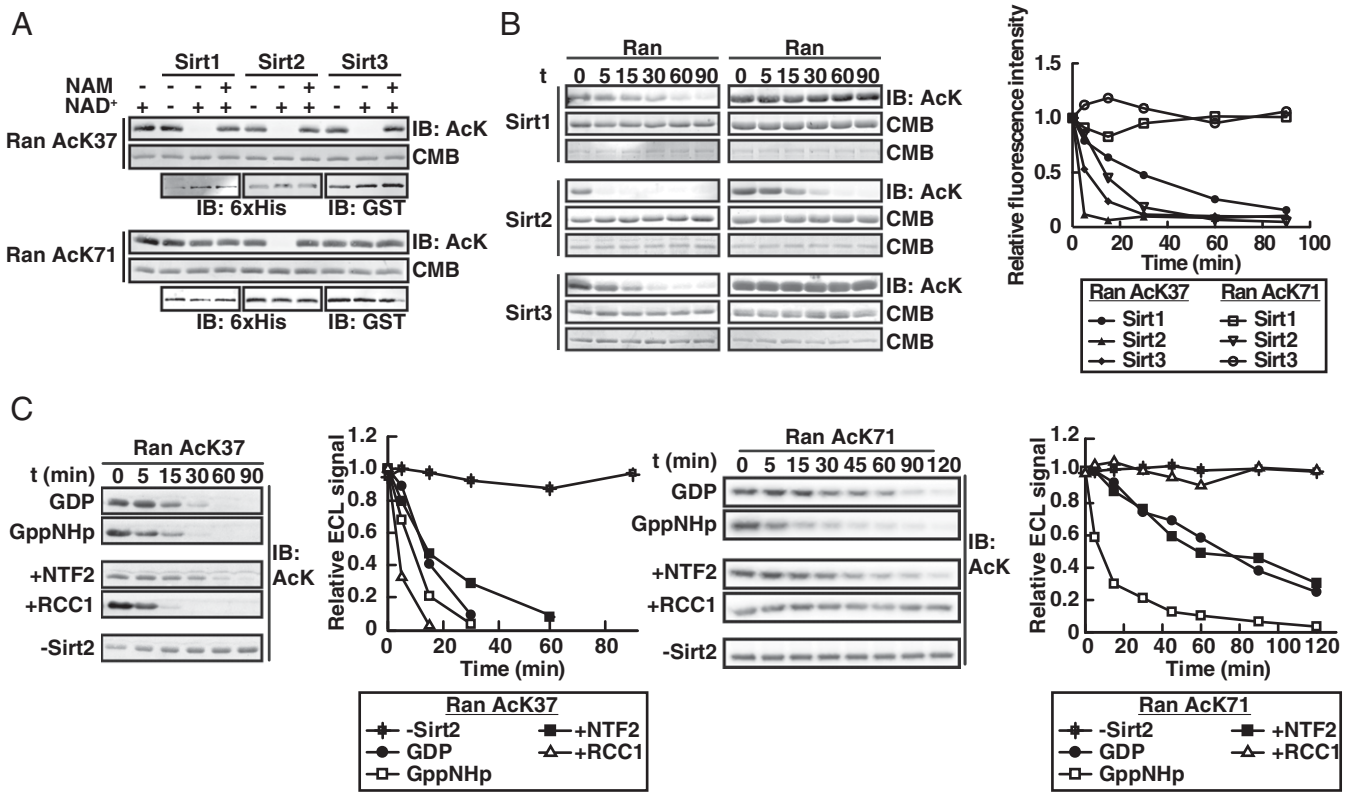

Fig. 5. Regulation of Ran acetylation by KDACs. (*A*) Ran AcK37 is deacetylated by Sirt1, -2, and -3, whereas Ran AcK71 is specifically deacetylated only by Sirt2. Three micrograms recombinant Ran was incubated with Sirt1, -2, and -3 (0.6, 0.2, and 0.55 μg) for 2 h at room temperature in the presence or absence of NAD^+ and nicotinamide (NAM). Shown are the immunoblots using the anti-AcK antibody after the in vitro deacetylase reaction. Coomassie (CMB) staining is shown as loading control for Ran AcK37, immunoblots using anti-His_6- and anti-GST antibodies for the sirtuins. (*B*) Kinetics of deacetylation of Ran AcK37 and Ran AcK71 by Sirt1, -2, and -3. Twenty-five micrograms recombinant Ran was incubated with Sirt1, -2, and -3 (4.5, 1.5, and 4.4 μg) depending on the individual enzyme activity (Fig. S4*B*). Shown is the immunoblot using the anti-AcK antibody (IB: AcK; *Left*) and the quantification of the time courses (*Right*). Ran AcK71 is only deacetylated by Sirt2; Ran AcK37 is deacetylated by all three sirtuins. (*C*) Dependence of Sirt2 deacetylation of Ran AcK37 and AcK71 on the nucleotide state and presence of the interactors NTF2 and RCC1. Sixty-five micrograms recombinant Ran was incubated with Sirt2 at 25 °C, and samples taken after the indicated time points. To compensate for the slower deacetylation rate, 3.7 μg Sirt2 was used for Ran AcK71, whereas only 1 μg Sirt2 was used for Ran AcK71. The immunodetection with the anti-AcK antibody and the corresponding quantification of the time course is shown. The deacetylation of Ran AcK37 depends on the nucleotide state; AcK71 is accelerated in the GppNHp-loaded state. Presence of NTF2 decelerates the deacetylation of Ran AcK37, whereas RCC1 accelerates it. For Ran AcK71, presence of NTF2 has no influence on the deacetylation kinetics by Sirt2; RCC1 blocks deacetylation. For loading and input controls of the time courses, please refer to Fig. S4*D*.

of interaction partners such as NTF2 and RCC1 influence Sirt2-catalyzed deacetylation (Fig. 5*C*). We observed that the deacetylation of Ran AcK37 by Sirt2 is independent of its nucleotide state, whereas Ran AcK71 deacetylation is considerably accelerated when GppNHp loaded. For Ran AcK37, the presence of NTF2 decelerates the deacetylation by Sirt2, whereas the presence of RCC1 accelerates it. AcK37 is not directly in the interface of the Ran•NTF2 (PDB ID code 1A2K) or the Ran•RCC1 (PDB ID code 1I2M) complex. The presence of NTF2 might sterically restrict access of Sirt2 to its substrate Ran AcK37. By contrast, RCC1 might increase the Sirt2 deacetylation rate by bringing switch I in a conformation more potent for deacetylation. As expected, RanAcK71 deacetylation is unaffected by the presence of NTF2 because AcK71 blocks the interaction with NTF2. RCC1 completely blocks Sirt2 deacetylation as AcK71 is within the RCC1-Ran interface and therefore protected from deacetylation.

Ran is acetylated by the KATs CBP, p300, Tip60, and α-TAT. To identify lysine acetyltransferases (KATs) that could potentially acetylate Ran, we performed an in vitro assay using commercially available (recombinantly expressed) KATs. Ran_{WT} protein was incubated with active full-length Tip60, Gcn5, CBP, and active p300 (aa 965–1810) and pCAF (KAT domain), and the reaction was analyzed by immunoblotting. The enzymatic activity of the used KATs was verified using histones H3/H4 as substrates (Fig. S5*A*). We obtained a Ran-specific acetylation signal for CBP and p300 (Fig. 6*A*). The reaction products were also analyzed by tryptic digest and MS to identify the acetylation sites. Several acetylation sites were found, which were predominantly identical for CBP and Tip60 (Fig. 6*B*). The volcano plot of three independent in vitro KAT assays with Ran_{WT} and CBP points out three acetylation sites with $P < 0.05$ (Fig. 6*C*). Thus, lysines 37, 134, and 142 of Ran appear to be the major acetyl acceptor residues for the two acetyl transferases CBP and Tip60 under the assay conditions in vitro.

As a second strategy, we also coexpressed 6xHis-Ran with the KATs in HEK-293T cells to find additional acetylation sites not found by the in vitro approach and to identify sites that could represent false positives. After coexpression, Ran acetylation was examined by Ni-NTA pulldown of 6xHis-Ran and subsequent MS analysis (Fig. S5*B*). Unexpectedly, although the α-tubulin acetyltransferase (α-TAT) has thus far been described as an exclusive KAT for α-tubulin, we found $K152^R$ acetylation on its overexpression. Moreover, overexpression of Tip60, CBP, and p300 resulted in an increased acetylation of $K134^R$ and CBP to an increase in $K142^R$ acetylation compared with the control (Fig. 6*D*), which is largely consistent with our in vitro data.

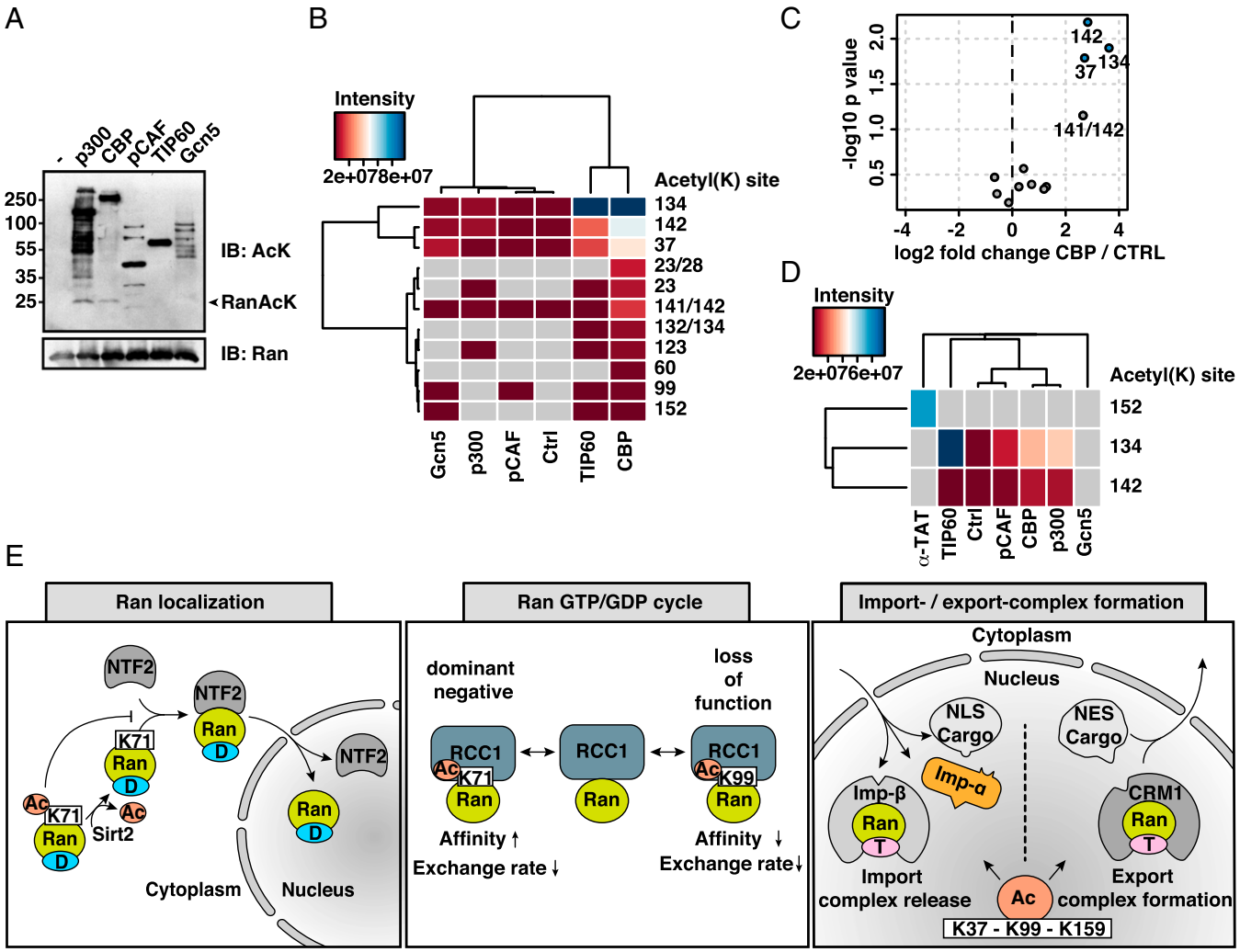

Fig. 6. Ran is acetylated by the KATs CBP and Tip60 in vitro and on KAT overexpression in cells. (*A*) Immunoblotting of the in vitro KAT assay of Ran using recombinant p300, CBP, pCAF, Tip60, and Gcn5. p300 and CBP acetylate Ran (anti-AcK). As loading control Ran was stained with an anti-Ran antibody. (*B*) Heat map with hierarchical clustering of identified acetylation sites. Increased Ran acetylation was detected for Tip60, CBP, and p300, predominantly at lysines 134, 142, and 37. The mean intensities of two independent in vitro KAT assays are shown. (*C*) Volcano plot of three independent in vitro KAT-assays with Ran and CBP. The Ran lysines 37, 134, and 142 were identified as the most significant acetylation sites ($P < 0.05$). (*D*) Heat map with hierarchical clustering of identified acetylation sites after transfection of KATs and subsequent Ni pulldown of Ran from HEK cells. Increased Ran acetylation at lysine 134 was detected for Tip60, CBP, and p300. Lysine 152 was exclusively acetylated by α-TAT. The mean intensities of two independent in vivo KAT assays are shown. (*E*) Working model of the regulation of Ran by posttranslational lysine acetylation. (*Left*) Ran acetylation at K71 abolishes NTF2 binding, thereby preventing nuclear Ran localization. Also, K99R does show cytosolic distribution by an unidentified mechanism. D, GDP. (*Center*) Ran acetylation at K71 and K99 affects the Ran•GDP/GTP cycle by interfering with RCC1-catalyzed nucleotide exchange and binding. AcK71 increases RCC1 binding and decreases RCC1 activity on Ran (dominant negative); AcK99 decreases RCC1 binding and RCC1 activity on Ran (loss of function). Furthermore, AcK71 decreases the intrinsic GTP hydrolysis rate. (*Right*) Ran acetylation at K37, K99, and K159 increases the affinity toward Importin-β and Spn1 if complexed with Crm1. Thereby, lysine acetylation might interfere with import substrate release and export substrate binding in the nucleus. T, GTP.

Taken together, our results with selected KATs suggest that CBP, p300, Tip60, and α-TAT can act as KATs for Ran, with $K37^R$, $K134^R$, $K141^R$, and $K152^R$ as the major acetyl acceptors. $K134^R$ has been implicated to be essential for the interaction with Mog1, a nuclear nucleotide release factor affecting nuclear protein import. In fact, acetylation of $K134^R$ abolishes binding toward Mog1 under the assay conditions used, whereas nonacetylated Ran binds with 7.5 μM affinity and a stoichiometry of 0.5 (Fig. 6) (37, 38).

Discussion

Here, we present an extensive study on the impact of lysine acetylation of the small GTPase Ran on protein function. We used site-specifically lysine-acetylated recombinant proteins to gain a comprehensive understanding of the impact of this modification for each site. Based on the whole proteome acetylation screen performed by Choudhary et al., we investigated five acetylation sites of Ran (K37, K60, K71, K99, and K159), some of which seemed very likely to alter Ran function, as judged by solved crystal structures (22). The presented in vitro characterization, combined with cell culture experiments, indicates a broad regulatory spectrum of Ran acetylation, influencing the Ran•GDP/GTP cycle, Ran localization, and import/export complex formation (see model in Fig. 6*E*).

Modification of lysine 71 abolishes NTF2 binding by disruption of two salt bridges to $D92^N$ and $D94^N$ of NTF2, consequently preventing nuclear Ran localization. Ran AcK71, furthermore, exhibits a dominant negative effect comparable to the $T24N^R$ mutation, increasing the RCC1-affinity while decreasing RCC1-catalyzed

nucleotide dissociation (39, 40). Moreover, it slightly increases the intrinsic nucleotide hydrolysis rate. Acetylation of Ran at K99 might also affect nuclear localization of Ran as shown by the $K99R^R$ mutant, independent from NTF2 binding via an unknown mechanism. The acetylation of lysine 99 results in a drastic reduction of the RCC1-catalyzed nucleotide exchange rate and it impairs RCC1 affinity (loss of function). This effect is accompanied by a different thermodynamic binding profile (less exothermic, more entropically favored) indicating an altered binding mechanism. Additionally, Ran AcK99 shows a nearly 34-fold reduced binding affinity to RanGAP if present in a complex with RanBP1 (see model in Fig. 6*E*).

Other acetylation sites ($K37^R$, $K99^R$, and $K159^R$) have the potential to influence binding affinities to import/export receptors or RanGAP. Acetylation of Ran at K37, K99, and K159 increases binding toward Importin-β predominantly due to a strong decrease in the complex dissociation rates. Moreover, acetylation of Ran at K37, K99, and K159 also increases the binding of Spn1 to a preformed CRM1•Ran•GppNHp complex. Having characterized the impact of Ran acetylation on the Crm1•Spn1 export complex and on the Importin-β interaction, we speculate that Ran acetylation could support import substrate release in the nucleus and enhance subsequent nuclear export cargo binding (see model in Fig. 6*E*).

The observed increasing/decreasing effects on binding affinities or interaction dynamics could be a means of fine regulation of cellular processes. However, the evaluation of the impact of these effects would need further studies in the physiological context. We conclude that an accumulation of acetylation would have drastic consequences for Ran localization, the formation of the cellular Ran•GTP/GDP gradient, and Ran-mediated import and export processes (Fig. 6*E*). Considering Ran as a representative, this also illustrates the broad regulatory spectrum and the strong possible impact of lysine acetylation in general.

Ran has been found to be ubiquitylated by MS. In fact, all sites that we studied here and the additional sites we found in our in vitro/in vivo KAT assays are targeted by ubiquitylation (41, 42). Moreover, succinylation of Ran has been detected in HeLa cells (lysines 23, 37, 99, 127, and 152) and mouse embryonic fibroblasts (lysines 23, 134, 142, and 159) (43, 44). Therefore, acetylation might directly cross-talk with ubiquitylation and lysine succinylation. Notably, further lysine acylation modifications, such as butyrylation, propionylation, malonylation, crotonylation, glutarylation, and myristoylation were discovered, many on histones (45, 46). If and to which extent Ran is modified by additional acylations remains to be elucidated. Future studies will show how the different acylations are regulated and how they differ mechanistically in regulating protein function.

Enzymatic regulation of lysine acetylation by KATs and KDACs is an indicator for physiological relevance. Therefore, we tested all human KDACs (classical and sirtuins) regarding their deacetylase activity toward the five Ran acetylation sites. Only Ran AcK37 and Ran AcK71 were identified as deacetylase substrates in vitro. Ran AcK71 is specifically deacetylated by Sirt2, whereas Ran AcK37 is a substrate for Sirt1, -2, and -3. Interestingly, in a recent peptide microarray assay, screening sirtuins 1–7 for activity toward all acetylated peptides derived from the Choudhary screen, Rauh et al. (47) did not detect any of the described activities. This failure might reflect that structural features could be important for substrate recognition by sirtuins. Moreover, we did observe that the five Ran acetylation sites give rise to considerably different signal intensities when detected with a pan-anti-acetyl-lysine (AcK) antibody, which is in line with observations by Rauh et al. and other groups (47, 48). This primary sequence dependence appears to be a common feature of pan-anti-AcK antibodies and thus has to be taken into account for the evaluation of proteomic screens with affinity-enriched material and quantitative immunoblots of complex protein samples.

We identified $K37^R$, $K134^R$, $K142^R$, and $K152^R$ as possible targets of p300, CBP, Tip60, and α-TAT in in vitro and/or overexpression studies. An analysis of available structural data shows that $K142^R$ is positioned toward the Importin-β and Crm1 Huntington, elongation factor 3, PR65/A, TOR (HEAT) repeat region (Table S2; PDB ID codes 1IBR, 2HB2, 3GJX, 3NC1, and 3NBY) (3, 12, 49, 50). Acetylation at this position might therefore interfere with import/export receptor binding. $K152^R$ is within the SAK/G5 motif known to be important for nucleotide binding by contacting the guanine base (51). Thus, $AcK152^R$ might affect the nucleotide binding on Ran. Moreover, $K152^R$ and $K37^R$ form direct salt bridges toward the Crm1 D436, located in the Crm1 intra-HEAT9 loop known to affect export substrate release (3, 49, 52). $K152^R$ and $K37^R$ also both intramolecularly contact the acidic Ran C-terminal $_{211}$DEDDDL$_{216}$ motif in the ternary complexes of Ran and RanGAP, as well as Ran, Crm1, and RanBP1 (Table S2; PDB ID codes 1K5D, 1K5G, and 4HAT) (50, 53). Therefore, acetylation might play a role in RanGAP-catalyzed nucleotide hydrolysis and export substrate release in the presence of RanBP1. $K134^R$ forms electrostatic interactions toward D364 and S464 in Crm1 but only in the complex of RanBP1 with Ran•GppNHp•Crm1, which would be abolished on acetylation (PDB ID code 4HB2) (50). Furthermore, $K134^R$ (K136 in yeast) was found to play an essential role for the interaction of yeast Ran and the nucleotide release factor Mog1 (37, 38). ITC measurements show that Ran K134 acetylation abolishes Mog1 binding under the conditions tested (Fig. S5*C*), which could indicate a regulatory function of this acetyl acceptor lysine.

Based on the in vitro activities of KATs and KDACs toward Ran we observed in this study, it is tempting to speculate about their possible roles in regulating Ran function. However, it is reported that KATs and classical KDACs are active in large multiprotein complexes, in which their activities are tightly regulated. Neither in vitro assays nor overexpression experiments can completely reproduce in vivo conditions, which makes it difficult to draw definite conclusions about the regulation of Ran acetylation in a physiological context. The limitations of these assays are to some extent also reflected by the fact that several additional Ran acetylation sites than those presented in this study can be found in available high-throughput MS data (23, 54). However, further studies are required to gain insight into the regulation of Ran function by lysine acetylation in vivo. These studies include the determination of the Ran acetylation stoichiometry under different physiological conditions, cell cycle states, and tissues.

Ran plays important roles in diverse cellular processes such as nucleo-cytoplasmic transport, mitotic spindle formation, and nuclear envelope assembly. These cellular functions are controlled by overlapping but also distinct pools of proteins. Lysine acetylation might represent a system to precisely regulate Ran function depending on the cellular process. The activity of acetyltransferases, deacetylases, the extent of nonenzymatic acetylation, and the availability of NAD^+ and acetyl-CoA may eventually determine the stoichiometry of intracellular Ran acetylation at a given time. This hypothesis would fit to the finding of a recent high-throughput MS screen showing that acetylation sites of Ran are often found in a tissue-specific manner (23). Notably, a high stoichiometry is not per se a prerequisite to be of physiological importance if acetylation creates a gain of function or if acetylation happens in a pathway of consecutive steps.

In summary, lysine acetylation affects many essential aspects of Ran protein function: Ran activation, inactivation, subcellular localization, and its interaction with import and export receptors. Although many publications deal with the pure identification and (semi)quantification of lysine acetylation, this study presents detailed mechanistic data of how acetylation affects protein function. Based on our results, we think of lysine acetylation as a potent system to regulate protein function. However, to understand the functions of acetylation in the physiological context, many open questions have to be resolved and challenges need to be overcome. A major challenge in the field of lysine acetylation and more general protein acylation will be to define the

physiological conditions under which these modifications exert their regulatory functions. Future studies are needed to understand the in vivo dynamics of acetylation, particularly under which cellular conditions specific sites are regulated and how the regulation of acetylation is coupled to the expression/activation of specific acetylation-regulating enzymes. Technological progress in proteomics enabling the absolute quantification of acetylation events in cells or tissues will be essential to address these questions. This study once more illustrates that combining the GCEC with in vitro characterization is a powerful strategy to investigate site-specific molecular effects of protein acetylation and might be a step further toward the development of more specific and more potent therapeutics targeting the acetylation/deacetylation machinery.

Materials and Methods

Incorporation of *N*-(ε)-Acetyl-Lysine. Acetyl-lysine-Ran (RanAcK) was expressed from a pRSF-Duet vector containing the coding regions for the synthetically evolved *Methanosarcina barkeri* MS $tRNA_{CUA}$ (*Mb*$tRNA_{CUA}$), the acetyl-lysyl-tRNA-sythetase, and the Ran containing an amber stop codon at the respective position of acetyl-lysine incorporation. The incorporation of acetyl-lysine in *E. coli* is directed by the acetyl-lysyl-tRNA synthetase (*Mb*PylRS) and its cognate amber suppressor, *Mb*$tRNA_{CUA}$, as response to an amber codon. The site-specific incorporation of *N*-(ε)-acetyl-lysine was done by supplementing the *E. coli* BL21 (DE3) cells with 10 mM *N*-(ε)-acetyl-lysine (Bachem) and 20 mM nicotinamide to inhibit the *E. coli* CobB deacetylase at an OD_{600} of 0.6 (37 °C). Cells were grown for another 30 min, and protein expression was induced by addition of 100–300 μM IPTG. After induction, the culture was grown 16 h at a reduced temperature of 20 °C and pelleted at 3,993 × *g* for 20 min. After resuspension in buffer D (25 mM Tris·HCl pH 8.0, 500 mM NaCl, 5 mM $MgCl_2$, 2 mM β–mercaptoethanol, 10 mM imidazole, 1:1,000 PMSF), sonication, and centrifugation (48,384 × *g*, 45 min), the lysate was applied to an equilibrated Ni-affinity column. The column-bound protein was washed extensively with high salt buffer (buffer D with 1 M NaCl). The protein was eluted, applying a gradient from 10 to 500 mM imidazole (25 mM Tris·HCl, pH 8.0, 300 mM NaCl, 5 mM $MgCl_2$, and 2 mM β-mercaptoethanol) over 10 column volumes. Fractions containing the target protein were pooled, concentrated, and applied to SEC (buffer C). Finally, the highly pure protein was concentrated, flash frozen, and stored at −80 °C.

Stopped Flow Kinetics. Stopped-flow experiments were done at 25 °C using a SX20 Applied Photophysics spectrometer. All stopped-flow measurements were done in buffer E (KP_i, pH 7.4, 5 mM $MgCl_2$, 2 mM β-mercaptoethanol). To determine RCC1-catalyzed nucleotide exchange rates, mant [2′/3′-O-(N-methylanthraniloyl)]-labeled Ran was excited at 295 nm, and the emission was recorded as a FRET-signal using a 420-nm cutoff filter. A constant concentration of 1 μM (final, 500 nM) Ran•mantGDP was titrated with increasing concentrations of RCC1 (0.039–80 μM; final: 0.0195–40 μM) in the presence of excess GTP (50 μM; final: 25 μM). The fluorescence signal was plotted over time and fitted to a single-exponential function to give the observed rates (k_{obs}) for each RCC1 concentration. The plot of the k_{obs} values over the RCC1 concentration resulted in a hyperbolic curve, which on fitting to a hyperbolic function resulted in the maximal rate of nucleotide dissociation, k_{-2} (29). The association of Ran•mantGppNHp and Importin-β was monitored by using an excitation of 350 nm and an emission cutoff filter of 420 nm; 200 nM (final 100 nM) of Ran•mantGppNHp was titrated with increasing concentrations of Importin-β (1–8 μM; final 0.5–4 μM). The increase in fluorescence was monitored over time and fitted to a single-exponential function to give the observed rates (k_{obs}). The plot of the k_{obs} values over the Importin-β concentration resulted in a linear curve with the slope k_{on}. GraFit 7.0 was used for data analysis.

KDAC Assays. Deacetylase assays were done in HDAC buffer (25 mM Tris, pH 8.0, 137 mM NaCl, 2.7 mM KCl, 1 mM $MgCl_2$, 0.1 mg/mL BSA, and 0.5 mM NAD^+). Acetylated Ran was incubated with catalytic amounts of KDACs for the indicated time at 25 °C. The reaction was stopped by adding sample buffer and heating the samples for 5 min at 95 °C. Acetylation was detected by immunoblotting with the anti-AcK antibody in 3% (wt/vol) milk.

KAT Assay. Ran (120 pmol) was incubated with 1 μL recombinant acetyltransferase (full-length: CBP, Gcn5, TIP60; p300, aa 965–1810, pCAF, 165 aa from HAT domain, activities as purchased from Biomol) in transferase buffer [50 mM Tris·HCl, 50 mM KCl, 5% (vol/vol) glycerol, 1 mM DTT, 0.1 mM EDTA, pH 7.3] supplemented with 100 μM acetyl-CoA for 4 h at 25 °C. The reaction was stopped by adding sample buffer and heating the samples for 5 min at 95 °C. Acetylation was detected by immunoblotting. Enzyme activities were tested using histone substrates (0.75 μg H3, 7.5 μg H4). For analysis by MS, 10 μg Ran_{WT} (10 μM in 40 μL) was incubated with 1 μL transferase in KAT buffer for 4 h at 25 °C.

Nucleotide Exchange. Nucleotide exchange on the small GTPase Ran was done in buffer C; 3–10 mg protein was incubated with a 5-fold (GppNHp and mant-labeled nucleotides) or 80-fold (GDP, GTP) molar excess of nucleotide in the presence of catalytic amounts of GST-RCC1. If a nonhydrolyzable nucleotide was to be loaded, 1 μL calf intestinal phosphatase (CIP; NEB) was added to the reaction to hydrolyze GDP/GTP. GST-RCC1 was removed with glutathione-Sepharose beads, and Ran was separated from excess nucleotide by SEC. Loading of Ran was verified by HPLC. All nucleotides were purchased from Jena Biosciences.

ITC Measurements. The interactions of Ran and acetylated Ran proteins and effectors/regulators (RCC1, Importin-β, CRM1, RanBP1, Mog1) were analyzed thermodynamically by ITC on an ITC_{200} instrument (GE Healthcare) based on Wiseman et al. (55). All measurements were done in buffer C or E. For a typical experiment, 2–3 μL of protein/peptide A in the syringe (0.1–700 μM) was injected into the cell containing protein B in concentrations of 10–140 μM depending on the interaction analyzed. The heating power per injection was plotted as a function of time until binding saturation was obtained. The binding isotherms were fitted to a one-site-binding model using the MicroCal software. This analysis yielded the stoichiometry of binding (N), the enthalpy change (ΔH), and the equilibrium-association constant (K_A) as direct readout from the experiments. ΔG, ΔS, and the equilibrium-dissociation constant (K_D) are derived. We used the standard EDTA-$CaCl_2$ sample tests as described by MicroCal to assess the statistical significance of individual observations. These measurements gave values within the manufacturer's tolerances of ±20% for K_A values and ±10% in ΔH. The data were analyzed using the software provided by the manufacturer.

ACKNOWLEDGMENTS. We thank Dr. Tobias Lamkemeyer, Astrid Wilbrand-Hennes, and René Grandjean [Cologne Excellence Cluster on Cellular Stress Responses in Aging-Associated Diseases (CECAD) proteomics facility] for support in mass spectrometry and Dr. Astrid Schauss and Dr. Nikolay Kladt (CECAD imaging facility) for critical and helpful discussions of the cell biological experiments. We are grateful to Prof. Dr. A. Wittinghofer and Dr. Ingrid Vetter for sending us Ran-constructs. Philipp Knyphausen was in part funded by International Graduate School in Development Health and Disease fellowship. This study was funded by the Emmy Noether Program of the German Research Foundation (Deutsche Forschungsgemeinschaft Grant LA2984-1/1).

1. Clarke PR, Zhang C (2008) Spatial and temporal coordination of mitosis by Ran GTPase. *Nat Rev Mol Cell Biol* 9(6):464–477.
2. Scheffzek K, Klebe C, Fritz-Wolf K, Kabsch W, Wittinghofer A (1995) Crystal structure of the nuclear Ras-related protein Ran in its GDP-bound form. *Nature* 374(6520): 378–381.
3. Monecke T, et al. (2009) Crystal structure of the nuclear export receptor CRM1 in complex with Snurportin1 and RanGTP. *Science* 324(5930):1087–1091.
4. Stewart M, Kent HM, McCoy AJ (1998) Structural basis for molecular recognition between nuclear transport factor 2 (NTF2) and the GDP-bound form of the Ras-family GTPase Ran. *J Mol Biol* 277(3):635–646.
5. Ren M, Drivas G, D'Eustachio P, Rush MG (1993) Ran/TC4: A small nuclear GTP-binding protein that regulates DNA synthesis. *J Cell Biol* 120(2):313–323.
6. Kalab P, Weis K, Heald R (2002) Visualization of a Ran-GTP gradient in interphase and mitotic Xenopus egg extracts. *Science* 295(5564):2452–2456.
7. Akhtar N, Hagan H, Lopilato JE, Corbett AH (2001) Functional analysis of the yeast Ran exchange factor Prp20p: In vivo evidence for the RanGTP gradient model. *Mol Genet Genomics* 265(5):851–864.
8. Ohtsubo M, Okazaki H, Nishimoto T (1989) The RCC1 protein, a regulator for the onset of chromosome condensation locates in the nucleus and binds to DNA. *J Cell Biol* 109(4 Pt 1):1389–1397.
9. Renault L, Kuhlmann J, Henkel A, Wittinghofer A (2001) Structural basis for guanine nucleotide exchange on Ran by the regulator of chromosome condensation (RCC1). *Cell* 105(2):245–255.
10. Monecke T, Dickmanns A, Ficner R (2014) Allosteric control of the exportin CRM1 unraveled by crystal structure analysis. *FEBS J* 281(18):4179–4194.
11. Hahn S, Schlenstedt G (2011) Importin β-type nuclear transport receptors have distinct binding affinities for Ran-GTP. *Biochem Biophys Res Commun* 406(3):383–388.
12. Vetter IR, Arndt A, Kutay U, Görlich D, Wittinghofer A (1999) Structural view of the Ran-Importin beta interaction at 2.3 A resolution. *Cell* 97(5):635–646.
13. Sarić M, et al. (2007) Structural and biochemical characterization of the Importin-beta.Ran.GTP.RanBD1 complex. *FEBS Lett* 581(7):1369–1376.
14. Cingolani G, Lashuel HA, Gerace L, Müller CW (2000) Nuclear import factors importin alpha and importin beta undergo mutually induced conformational changes upon association. *FEBS Lett* 484(3):291–298.

15. Cingolani G, Petosa C, Weis K, Müller CW (1999) Structure of importin-beta bound to the IBB domain of importin-alpha. *Nature* 399(6733):221–229.
16. Bischoff FR, Görlich D (1997) RanBP1 is crucial for the release of RanGTP from importin beta-related nuclear transport factors. *FEBS Lett* 419(2-3):249–254.
17. Lounsbury KM, Macara IG (1997) Ran-binding protein 1 (RanBP1) forms a ternary complex with Ran and karyopherin beta and reduces Ran GTPase-activating protein (RanGAP) inhibition by karyopherin beta. *J Biol Chem* 272(1):551–555.
18. Monecke T, et al. (2013) Structural basis for cooperativity of CRM1 export complex formation. *Proc Natl Acad Sci USA* 110(3):960–965.
19. Wong DH, Corbett AH, Kent HM, Stewart M, Silver PA (1997) Interaction between the small GTPase Ran/Gsp1p and Ntf2p is required for nuclear transport. *Mol Cell Biol* 17(7):3755–3767.
20. Ribbeck K, Lipowsky G, Kent HM, Stewart M, Görlich D (1998) NTF2 mediates nuclear import of Ran. *EMBO J* 17(22):6587–6598.
21. Yang MH, et al. (2012) Regulation of RAS oncogenicity by acetylation. *Proc Natl Acad Sci USA* 109(27):10843–10848.
22. Choudhary C, et al. (2009) Lysine acetylation targets protein complexes and co-regulates major cellular functions. *Science* 325(5942):834–840.
23. Lundby A, et al. (2012) Proteomic analysis of lysine acetylation sites in rat tissues reveals organ specificity and subcellular patterns. *Cell Reports* 2(2):419–431.
24. Beli P, et al. (2012) Proteomic investigations reveal a role for RNA processing factor THRAP3 in the DNA damage response. *Mol Cell* 46(2):212–225.
25. Chen Y, et al. (2012) Quantitative acetylome analysis reveals the roles of SIRT1 in regulating diverse substrates and cellular pathways. *Mol Cell Proteomics* 11(10): 1048–1062.
26. Mertins P, et al. (2013) Integrated proteomic analysis of post-translational modifications by serial enrichment. *Nat Methods* 10(7):634–637.
27. Neumann H, Peak-Chew SY, Chin JW (2008) Genetically encoding N(epsilon)-acetyllysine in recombinant proteins. *Nat Chem Biol* 4(4):232–234.
28. Lammers M, Neumann H, Chin JW, James LC (2010) Acetylation regulates cyclophilin A catalysis, immunosuppression and HIV isomerization. *Nat Chem Biol* 6(5):331–337.
29. Klebe C, Prinz H, Wittinghofer A, Goody RS (1995) The kinetic mechanism of Ran—nucleotide exchange catalyzed by RCC1. *Biochemistry* 34(39):12543–12552.
30. Renault L, et al. (1998) The 1.7 A crystal structure of the regulator of chromosome condensation (RCC1) reveals a seven-bladed propeller. *Nature* 392(6671):97–101.
31. Klebe C, Bischoff FR, Ponstingl H, Wittinghofer A (1995) Interaction of the nuclear GTP-binding protein Ran with its regulatory proteins RCC1 and RanGAP1. *Biochemistry* 34(2):639–647.
32. Seewald MJ, et al. (2003) Biochemical characterization of the Ran-RanBP1-RanGAP system: Are RanBP proteins and the acidic tail of RanGAP required for the Ran-RanGAP GTPase reaction? *Mol Cell Biol* 23(22):8124–8136.
33. Villa Braslavsky CI, Nowak C, Görlich D, Wittinghofer A, Kuhlmann J (2000) Different structural and kinetic requirements for the interaction of Ran with the Ran-binding domains from RanBP2 and importin-beta. *Biochemistry* 39(38):11629–11639.
34. Kutay U, Bischoff FR, Kostka S, Kraft R, Görlich D (1997) Export of importin alpha from the nucleus is mediated by a specific nuclear transport factor. *Cell* 90(6):1061–1071.
35. Smith A, Brownawell A, Macara IG (1998) Nuclear import of Ran is mediated by the transport factor NTF2. *Curr Biol* 8(25):1403–1406.
36. Dong X, et al. (2009) Structural basis for leucine-rich nuclear export signal recognition by CRM1. *Nature* 458(7242):1136–1141.
37. Baker RP, Harreman MT, Eccleston JF, Corbett AH, Stewart M (2001) Interaction between Ran and Mog1 is required for efficient nuclear protein import. *J Biol Chem* 276(44):41255–41262.
38. Steggerda SM, Paschal BM (2000) The mammalian Mog1 protein is a guanine nucleotide release factor for Ran. *J Biol Chem* 275(30):23175–23180.
39. Kornbluth S, Dasso M, Newport J (1994) Evidence for a dual role for TC4 protein in regulating nuclear structure and cell cycle progression. *J Cell Biol* 125(4):705–719.
40. Dasso M, Seki T, Azuma Y, Ohba T, Nishimoto T (1994) A mutant form of the Ran/TC4 protein disrupts nuclear function in Xenopus laevis egg extracts by inhibiting the RCC1 protein, a regulator of chromosome condensation. *EMBO J* 13(23):5732–5744.
41. Wagner SA, et al. (2011) A proteome-wide, quantitative survey of in vivo ubiquitylation sites reveals widespread regulatory roles. *Molec Cell Proteomics* 10(10): M111.
42. Wagner SA, et al. (2012) Proteomic analyses reveal divergent ubiquitylation site patterns in murine tissues. *Mol Cell Proteomics* 11(12):1578–1585.
43. Weinert BT, et al. (2013) Lysine succinylation is a frequently occurring modification in prokaryotes and eukaryotes and extensively overlaps with acetylation. *Cell Reports* 4(4):842–851.
44. Park J, et al. (2013) SIRT5-mediated lysine desuccinylation impacts diverse metabolic pathways. *Mol Cell* 50(6):919–930.
45. Xie Z, et al. (2012) Lysine succinylation and lysine malonylation in histones. *Mol Cell Proteomics* 11(5):100–107.
46. Liu B, et al. (2009) Identification and characterization of propionylation at histone H3 lysine 23 in mammalian cells. *J Biol Chem* 284(47):32288–32295.
47. Rauh D, et al. (2013) An acetylome peptide microarray reveals specificities and deacetylation substrates for all human sirtuin isoforms. *Nat Commun* 4:2327.
48. Zerweck J, Masch A, Schutkowski M (2009) Peptide microarrays for profiling of modification state-specific antibodies. *Methods Mol Biol* 524:169–180.
49. Güttler T, et al. (2010) NES consensus redefined by structures of PKI-type and Rev-type nuclear export signals bound to CRM1. *Nat Struct Mol Biol* 17(11):1367–1376.
50. Sun Q, et al. (2013) Nuclear export inhibition through covalent conjugation and hydrolysis of Leptomycin B by CRM1. *Proc Natl Acad Sci USA* 110(4):1303–1308.
51. Vetter IR, Wittinghofer A (2001) The guanine nucleotide-binding switch in three dimensions. *Science* 294(5545):1299–1304.
52. Koyama M, Matsuura Y (2010) An allosteric mechanism to displace nuclear export cargo from CRM1 and RanGTP by RanBP1. *EMBO J* 29(12):2002–2013.
53. Seewald MJ, Körner C, Wittinghofer A, Vetter IR (2002) RanGAP mediates GTP hydrolysis without an arginine finger. *Nature* 415(6872):662–666.
54. Choudhary C, Weinert BT, Nishida Y, Verdin E, Mann M (2014) The growing landscape of lysine acetylation links metabolism and cell signalling. *Nat Rev Mol Cell Biol* 15(8): 536–550.
55. Wiseman T, Williston S, Brandts JF, Lin LN (1989) Rapid measurement of binding constants and heats of binding using a new titration calorimeter. *Anal Biochem* 179(1):131–137.
56. R Core Team (2014) *R: A Language and Environment for Statistical Computing* (R Foundation for Statistical Computing, Vienna).